Published in final edited form as:

Cancer Res. 2018 August 01; 78(15): 4241–4252. doi:10.1158/0008-5472.CAN-17-3623.

Macrophages Promote Circulating Tumor Cell-Mediated Local Recurrence Following Radiation Therapy in Immunosuppressed Patients

Marjan Rafat[1], **Todd A. Aguilera**[2], **Marta Vilalta**[1], **Laura L. Bronsart**[1], **Luis A. Soto**[1], **Rie von Eyben**[1], **Meghana A. Golla**[1], **Yasaman Ahrari**[1], **Stavros Melemenidis**[1], **Anosheh Afghahi**[3], **Melissa J. Jenkins**[1], **Allison W. Kurian**[3], **Kathleen C. Horst**[1], **Amato J. Giaccia**[1], and **Edward E. Graves**[1,*]

[1]Department of Radiation Oncology, Stanford University, Stanford, CA 94305, USA

[2]Department of Radiation Oncology, Harold C. Simmons Comprehensive Cancer Center, U.T. Southwestern Medical Center, Dallas, TX 75390, USA

[3]Department of Medicine, Stanford University School of Medicine, Stanford, CA 94305 USA

Abstract

Although radiation therapy (RT) decreases the incidence of locoregional recurrence in breast cancer, patients with triple-negative breast cancer (TNBC) have increased risk of local recurrence following breast-conserving therapy (BCT). The relationship between RT and local recurrence is unknown. Here we tested the hypothesis that recurrence in some instances is due to the attraction of circulating tumor cells to irradiated tissues. To evaluate the effect of absolute lymphocyte count on local recurrence after RT in TNBC patients, we analyzed radiation effects on tumor and immune cell recruitment to tissues in an orthotopic breast cancer model. Recurrent patients exhibited a prolonged low absolute lymphocyte count when compared to non-recurrent patients following RT. Recruitment of tumor cells to irradiated normal tissues was enhanced in the absence of $CD8^+$ T cells. Macrophages ($CD11b^+F480^+$) preceded tumor cell infiltration and were recruited to tissues following RT. Tumor cell recruitment was mitigated by inhibiting macrophage infiltration using maraviroc, an FDA-approved CCR5 receptor antagonist. Our work poses the intriguing possibility that excessive macrophage infiltration in the absence of lymphocytes promotes local recurrence after RT. This combination thus defines a high-risk group of TNBC patients.

Keywords

Breast cancer; Cell motility and migration; Lymphokines; cytokines; chemokines; growth factors; Normal tissue response to radiation; Tumor microenvironment and modification

*Corresponding author: Edward E. Graves, Center for Clinical Sciences Research, Rm. 1260, Stanford University, Stanford, CA 94305. Phone: (650) 723-5591, Fax: (650) 498-4015, egraves@stanford.edu.

Conflicts of Interest

The authors declare no potential conflicts of interest.

Introduction

Understanding the conditions for locoregional recurrence following therapy in breast cancer patients is critical, particularly for triple negative breast cancer (TNBC) patients who are more likely to be younger and have worse outcomes (1). TNBC, which is treated with mastectomy or lumpectomy followed by radiation to the surgical cavity, is associated with reduced breast cancer-specific and overall survival, higher incidence of locoregional recurrence, and greater distant metastatic potential (2). Locoregional recurrence, despite aggressive local treatment with surgery and radiation, poses serious clinical challenges and has been linked to poor overall survival in TNBC patients (3–7). Therefore, understanding cellular and immune factors that contribute to locoregional recurrence in TNBC is essential to improving patient survival.

An emerging risk factor for worse overall survival in breast cancer patients is lymphopenia or reduced lymphocyte count; it is observed in approximately 20% of untreated metastatic breast cancer patients (8). Associated with a poor clinical outcome, lymphopenia can be caused not only by the myeloablative effects of many chemotherapies, but it can also be induced by radiotherapy (RT) (9). Post-RT lymphopenia has been shown to correlate with increased risk of death in TNBC patients (10). RT is generally administered following breast-conserving therapy (BCT) to reduce the risk of locoregional recurrence. RT is also indicated for patients receiving mastectomy who show signs of lymph node involvement, skin invasion, or positive surgical margins. In these clinical scenarios, RT reduces tumor recurrence in the breast by 50% as compared to surgery alone and ultimately improves overall survival if the recurrence risk reduction is sufficient (11). However, the impact of RT on local recurrence in a lymphopenic setting has largely been unstudied.

While local recurrence is typically thought to be due to failure at the treatment site, local recurrence may be facilitated by circulating tumor cell re-seeding of treated sites. We previously demonstrated that radiation enhances tumor cell recruitment (12). We hypothesized that lymphopenia may contribute to local recurrence by facilitating tumor re-seeding. We tested this hypothesis by first analyzing the absolute lymphocyte count (ALC) of TNBC patients following RT as part of their primary management, which revealed a previously unreported correlation between prolonged low lymphocyte count and local recurrence. Without further information about lymphocyte subtypes in patients, we then studied the effects of radiation on tumor cell recruitment in a murine model of TNBC in the absence of specific lymphocyte subtypes. Because RT is administered after tumor resection in patients and normal tissue is not spared during RT (13), we then evaluated how normal tissue radiation response modulates recurrence after therapy in an immunocompromised setting. We found that, in the absence of functional T cells, RT enhances recruitment of tumor cells from the circulation as well as inflammatory macrophages. We defined a novel role for lymphocytes, particularly $CD8^+$ T cells, in limiting macrophage-mediated tumor seeding of irradiated tissues, thereby explaining one of the mechanisms by which lymphopenia can contribute to poor outcomes. Our work highlights the importance of evaluating breast cancer subtype, patient immune competence, and disease dissemination to identify breast cancer patients who will be at risk for locoregional relapse.

Materials and Methods

Patient study

All studies using electronic medical records from Stanford University were approved by the Institutional Review Board (IRB), which deemed this retrospective analysis appropriate for a waiver of informed consent. These studies were conducted in accordance with the Declaration of Helsinki and the Belmont Report. Patients who were diagnosed with primary breast cancer and who received radiation to the breast for primary disease following surgery and chemotherapy were compiled by the Stanford Cancer Institute Research Database (SCIRDB) and the Stanford Oncoshare Project Database (14, 15). TNBC patients were evaluated for locoregional recurrence, which was defined as recurrence in the ipsilateral breast, chest wall, or ipsilateral draining lymph nodes. ALC for all patients were analyzed from 1 to 5 months after RT, and ROC analysis and the yoden criterion were used to select a 1.3K/μL cutoff point for distinguishing low ALC. Cumulative Recurrence free survival (RFS) was determined using the Kaplan Meier method with univariate comparisons between groups using the log-rank test.

Cell lines

Luciferase-labeled 4T1 mouse mammary carcinoma cells were obtained from Dr. Christopher Contag (Stanford University) in August 2011. MDA-MB-231 human breast cancer parental cells were obtained from Dr. Amato Giaccia (Stanford University) in August 2011. MDA-MB-231 cells were transduced with retrovirus particles encoding for the expression of firefly luciferase gene. Primary mouse embryonic fibroblasts (MEFs) were obtained from Dr. Laura Attardi (Stanford University) in November 2015. All cells were cultured at 37°C and 5% CO_2. 4T1 cells were cultured in in RPMI-1640 (Gibco) while MDA-MB-231 and MEFs were cultured in DMEM (Gibco), and both were supplemented with 10% FBS and antibiotics (100U/mL penicillin and 100mg/mL streptomycin). All cell lines tested negative for *Mycoplasma* contamination with the MycoAlert Mycoplasma Detection Kit (Lonza) in 2015. Cells were used within three passages before injection into mice.

Orthotopic tumor inoculation

Animal studies were performed in accordance with institutional guidelines and protocols approved by the Stanford University Institutional Animal Care and Use Committee. Tumor inoculation was performed by injecting 5×10^4 4T1 or 1×10^6 MDA-MB-231 cells in a volume of 50μL directly into the number 4 right mammary fat pads of 8–10 week old female BALB/c (4T1 only) or Nu/Nu (4T1, MDA-MB-231) mice. In T cell depletion experiments, 0.5mg anti-CD4 (GK1.5, BioXCell) and/or 0.5mg anti-CD8a (2.43, BioXCell) was injected intraperitoneally every 5 days starting from the day of inoculation (16). Control mice were injected with 0.5mg rat IgG2b isotype control (LTF-2, BioXCell) using the same dosing schedule. In macrophage migration inhibition experiments, 0.25mg maraviroc (Sigma) in PBS was injected daily intraperitoneally starting from 12 hours prior to radiation (17). Local CCL4 blocking experiments were done by injecting 50μg αCCL4 or isotype control into the contralateral MFP of Nu/Nu mice every 3 days starting from 12 hours prior to radiation (R&D Systems) (18, 19). Macrophage depletion experiments were done by administering

100 μL clodronate (5 mg/mL) or control liposomes intravenously to Nu/Nu mice every 2 days beginning 12 hours prior to radiation (clodronateliposomes.com) (20). All mice were purchased from Charles River Laboratories. Tumor length and width were measured twice weekly using digital calipers (Fisher Scientific) beginning at day 8 post-inoculation. Tumor volume was calculated using the formula Volume=$(D_1^2 x D_2)/2$, where D_1 is the minimum diameter and D_2 is the maximum diameter.

Radiation

Mouse MFPs were irradiated using a 250kVp cabinet x-ray system filtered with 0.5mm Cu. Mice were anesthetized by administering 80mg/kg ketamine hydrochloride and 5mg/kg xylazine intraperitoneally and then shielded using a 3.2mm lead jig with 1cm circular apertures to expose normal MFPs. Transmission through the shield was less than 1%.

Bioluminescence imaging

All bioluminescence imaging (BLI) was done at the Stanford Small Animal Imaging Facility. Mice bearing luciferase-expressing tumors were injected intraperitoneally with 3.3mg D-luciferin (Biosynth Chemistry & Biology) in PBS 10 minutes prior to imaging. Mice were anesthetized with isoflurane and bioluminescence was evaluated using the IVIS 200 imaging system (PerkinElmer). *Ex vivo* imaging was performed after euthanizing mice and harvesting tissues.

Invasion and chemotaxis assays

Conditioned media (CM) from MEFs and bone marrow-derived macrophages (BMDM) were used as chemoattractants in an *in vitro* transwell invasion assay (BD Biocoat Growth Factor Reduced Matrigel Invasion Chamber, 8μm pore size). MEFs were irradiated to 20 Gy using a Cesium source. Supernatant was collected after 2 or 7 days incubation to investigate tumor cell invasion. BMDM from Nu/Nu and BALB/c mice were harvested using previously established protocols (21). Briefly, bone marrow cells were isolated from the femurs of either Nu/Nu or BALB/c mice and placed in IMDM medium with 10% FBS and 10 ng/mL of MCSF for 7d for maturation into macrophages. CM from 2×10^6 mature BMDM was collected every 48 hours for 6 days. 1×10^5 4T1 cells were placed in the upper chambers and incubated with the CM for 24 hours. In BMDM CM experiments, the mouse CCL4 neutralizing antibody and the rat IgG2A isotype control (3 μg/ml, R&D Systems) were added to the media to determine the effect of blocking CCL4 on 4T1 cell invasion and chemotaxis. Recombinant CCL4 was also added to growth media to determine whether CCL4 can enhance 4T1 invasion (20 ng/mL, Peprotech) (22). Cells that invaded through the Matrigel inserts were stained using either crystal violet (0.25% in 95% methanol) or 4′,6-diamidino-2-phenylindole (DAPI) and counted. Chemotaxis was measured by imaging the 4T1 cells that migrated through the membrane to the 24 well receiver plate using BLI.

Luminex multiplex cytokine assay

MEFs were cultured in 6 cm dishes with 500,000 cells. Media was changed to DMEM with 2% FBS after 24 hours, and cells were irradiated to 20 Gy. Supernatant was collected after 7 days, filtered (0.2μm), concentrated with an Amicon Ultra Centrifugal filter (3kDa cutoff,

Millipore), and stored at −80°C until processed. 3 replicates were collected independently. MFPs of Nu/Nu and BALB/c mice were resected, placed in serum free RPMI with 0.1% bovine serum albumin, and irradiated to 20 Gy *ex vivo* (n = 7). CM was collected after 48 hours, filtered, and stored at −80°C until processed. CM was also collected from 2×10^6 BMDM every 48 hours for 6 days and stored at −80°C until processed. For *in* vivo studies, blood plasma from immunocompetent ($CD8^+$), immunocompromised ($CD8^-$), and maraviroc-treated mice ($CD8^-$) was collected 10 days following RT. All samples were processed at the Stanford Human Immune Monitoring Center using a mouse 38-plex Affymetrix kit.

Immunohistochemistry

Tissues were removed from mice and placed in 10% formalin for 24 hours at 4°C and then in 70% ethanol before embedding in paraffin and sectioning. Sections (4μm) were deparaffinized in xylene, rehydrated, boiled in citric acid (10mM, pH 6) for antigen retrieval, and treated with 3% hydrogen peroxide. Blocking in 10% goat serum was followed by incubation overnight at 4°C with anti-F4/80 (1:250, Abcam) and CD8 (1:100, eBioscience) primary antibodies. Sections were incubated with biotinylated secondary antibodies followed by incubation with the substrate using the DAB Peroxidase substrate kit (Vector Laboratories) and then counterstained with hematoxylin. A corresponding no primary antibody control was performed for all conditions to confirm specificity. Samples were imaged using an upright Leica microscope.

Flow cytometry

Flow cytometry analysis for this project was done on instruments in the Stanford Shared FACS Facility. Tissues were harvested, minced in media with 2.5% FBS, and placed in a solution of 200U/mL Type 1 collagenase (Worthington Biochemical Corporation) and 0.5U/mL dispase (Stemcell Techonologies) for 40 minutes at 37°C. Cells were strained through a 40μm mesh and resuspended in ACK Lysis Buffer for 5 minutes at room temperature (Quality Biological) to remove RBCs. Cells were stained with the Zombie NIR fixable viability stain (Biolegend), fixed on ice in 5% formalin buffered saline for 20 minutes, and frozen at −80°C before staining for cell surface markers. FC receptors were blocked with CD16/32 (Biolegend), and cells were stained with conjugated antibody cocktails for 20 minutes on ice. Flow cytometry was performed on an in-house four-laser machine, and FlowJo software was used for analysis. Compensations were obtained using compensation beads (Life Technologies). The following antibody clones (Biolegend) were used for analysis: CD45(30-F11), CD4(GK1.5), CD8(53-6.7), CD11b(M1/70), and F4/80(BM8).

Statistical analysis

To determine statistical significance, BLI data were analyzed in a general linear model (ANOVA). Post hoc analyses were performed with a Tukey adjustment for multiple comparisons. Dose dependence was evaluated using a generalized linear model (GLM) fit. Fisher's exact test was used for comparing non-recurrent to recurrent patient ALCs. The log-rank test was used to determine statistical significance in Kaplan-Meier analysis. Two-tailed

unpaired t-tests were used to establish statistical significance in immunohistochemistry (IHC) cell counts. All analyses were performed using SAS9.4 or GraphPad Prism 6.

Results

Correlation between low absolute lymphocyte count and locoregional recurrence in TNBC patients following RT

To determine if the absolute lymphocyte count (ALC) correlates with outcome, we examined the charts of 83 TNBC patients during the 5 months following RT. There were 15 patients with locoregional recurrence in the radiation field. The median follow-up time was 53 and 82 months in recurrent and non-recurrent groups, respectively. Table 1 delineates patient and tumor characteristics, and Supplementary Table S1 describes patient chemotherapy and radiation conditions. Receiver operating characteristic (ROC) analysis comparing recurrent and non-recurrent ALCs from month 1 to 5 post radiation helped define a cut off of 1300 counts per μL (1.3K/μL). This value for low lymphocyte count is consistent with previously published thresholds that define counts from less than 1 to 1.5K/μL as low ALC or lymphopenia (8, 23). RFS at 5 years for patients with 5 months of sustained low ALC 1 to 5 months after RT was 61% compared with 98% for patients with normal ALC ($p<0.0001$; Fig. 1A). We found that 14 of 15 (93%) patients with recurrence had persistently low ALC after radiation, whereas 45 of 68 (66%) of those patients without recurrence had recovery of their ALC in the 5 months following RT ($p<0.0001$; Fig. 1B). Fig. 1C shows the change in ALCs over time, revealing that recurrent patients exhibited sustained low lymphocyte count following RT while non-recurrent patient lymphocyte counts steadily increased after a nadir at 2 months post treatment ($p=0.0006$). The recurrent patients exhibited lower lymphocyte counts two months prior to RT compared to the non-recurrent patients. While this difference may be a possible indication for how immunodeficiency affects prognosis, we focused on the patients' inability to produce competent lymphocyte levels by modeling recurrence in mice with low lymphocyte levels before RT. There was no statistical difference in white blood cell count, absolute neutrophil count, or absolute monocyte count between the groups, suggesting that ALC within the period shortly following treatment is the most important factor in determining local recurrence risk (Fig. 1D–F).

Tumor cell recruitment to irradiated tissues

To study the contribution of low lymphocyte count on recurrence, the highly metastatic luciferase-expressing 4T1 murine and MDA-MB-231 human TNBC tumor cells were used as donors of circulating tumor cells for the seeding of radiated tissue in immunocompromised Nu/Nu mice. Once mammary fat pad (MFP) tumors reached a volume of 100 mm^3, the contralateral uninoculated MFPs were irradiated with 20 Gy (Fig. 2A), a dose consistent with what has been applied to human breast cancer patients both intraoperatively and postoperatively. 4T1 cell recruitment was evaluated after 10 days using *ex vivo* bioluminescence imaging (BLI) of tissues in the radiation field, including the MFP, peritoneum (Per), and muscle (Mus) (Fig. 2B). Tumor cell recruitment was observed in all tissues ($p<0.001$; Fig. 2C). BLI of the upper MFPs (UFPs) outside of the radiation field showed no differences in signal between irradiated and non-irradiated mice, demonstrating the specificity of tumor cell recruitment to irradiated sites as opposed to distant sites (Fig.

2D). Recruitment of MDA-MB-231 cells was also observed 10 days following RT, and UFPs also showed no differences in signal between irradiated and non-irradiated mice ($p<0.001$; Fig. 2E and 2F). MFPs resected from mice 10 days following RT were then incubated in complete media and *ex vivo* BLI analysis showed increased luminescence over time, verifying the presence of viable tumor cells (Supplementary Fig. S1). In addition, the extent of tumor cell recruitment was dose dependent in all tissues studied (Supplementary Fig. S2).

Unlike Nu/Nu mice, tumor cell recruitment to irradiated tissues was not observed in immunocompetent BALB/c mice, suggesting that the presence of functional lymphocytes suppress tumor seeding (Fig. 3A). There was also no difference between the UFPs of control and irradiated mice (Fig. 3B). Primary tumor growth was not affected by irradiating contralateral normal MFPs in immunocompromised or immunocompetent models (Fig. 3C; Supplementary Fig. S3A and S3B).

To model patients with low ALCs in immunocompetent mice, T cell populations were depleted using antibodies to CD4 and CD8. Following T cell depletion in BALB/c mice, the luminescent signal in irradiated MFPs was significantly increased ($p<0.05$; Fig. 3D and 3E). To determine which T cell population was critical for inhibiting tumor cell recruitment to irradiated tissue, we depleted $CD4^+$ and $CD8^+$ T cells individually. Depleting either individually enhanced tumor cell recruitment, but depleting $CD8^+$ T cells alone enhanced tumor cell recruitment to a greater extent than depleting $CD4^+$ T cells ($p<0.01$). This effect was not enhanced when depleting both populations simultaneously, indicating that $CD8^+$ T cells play the predominant role in inhibiting tumor cell recruitment to irradiated tissue. There were no significant differences in the luminescent signal between the UFPs of irradiated and unirradiated T cell depleted mice, suggesting that tumor cell recruitment is a localized effect of radiation (Fig. 3F). Tumor cell recruitment kinetics were examined using BLI, revealing that tumor cells were not recruited to normal tissues until 10 days post-RT (Fig. 3G–I). Primary tumor growth was also monitored, and no significant changes were observed when irradiating normal tissues or depleting T cell populations (Supplementary Fig. S3C and S3D). Lung metastatic lesions were analyzed to determine the effect of RT on altering CTC levels in Nu/Nu and BALB/c mice (Supplementary Fig. S3E and S3F). No significant differences in BLI signal were observed under any condition, suggesting that RT or $CD8^+$ T cell levels do not impact overall CTC dynamics. T cell depletion was confirmed using flow cytometry (Supplementary Fig. S4A–C).

Overall mouse health after RT was also examined (Supplementary Fig. S5A and S5B). Non-tumor bearing BALB/c mice were irradiated in the MFP, and complete blood counts and weight were monitored. While RT induced a modest reduction in lymphocyte levels consistent with our clinical data, monocyte count was not altered after 10 days (Supplementary Fig. S5A). In addition, MFP RT induced localized gut toxicity as expected since the GI tract was partially in the field of radiation. Toxicity was determined by a board-certified veterinary pathologist. However, this did not result in overall morbidity, and mouse weight loss over the course of the experiment showed that the radiation was well-tolerated as the mice did not lose more than 10% of their initial body weight (Supplementary Fig. S5B).

Immune cell infiltration in irradiated normal tissues

We hypothesized that radiation of normal tissue induces chemotactic factors that contribute to tumor cell recruitment. To test this, primary MEFs were irradiated with 20 Gy, and conditioned media was collected to be used in an *in vitro* transwell assay. We found that the conditioned media from irradiated MEFs enhanced tumor cell invasion of both luciferase-expressing 4T1 and MDA-MB-231 cells (Supplementary Fig. S6A and S6B). The luminex multiplex assay was performed to determine which cytokines or chemokines from the irradiated MEFs may contribute to tumor cell recruitment following RT (Supplementary Fig. S6C). Chemokines CCL3, CCL4, and CCL5 were the most highly induced factors following irradiation, which all interact with C-C chemokine receptor type 5 (CCR5) (24). Secretion of CCL3, 4, and 5 has been shown to alter macrophage and monocyte dynamics and migration (25). These chemokines contribute not only to macrophage and lymphocyte recruitment but also to the progression and metastatic potential of tumors (26). In addition, MFPs from Nu/Nu and BALB/c mice were resected and irradiated to 20 Gy *ex vivo*. CCL3 and CCL4 were enhanced 1.2 to 1.6-fold compared to unirradiated controls, which confirms the importance of the CCR5-axis in normal tissue radiation response (Supplementary Fig. S6D).

Because inflammatory chemokines involved in tumor and immune cell recruitment were enhanced in MEFs and MFPs following RT, we investigated how infiltrating immune cells influence tumor cell recruitment. We performed IHC staining of irradiated mouse tissues for $CD8^+$ T cells and $F4/80^+$ macrophages. We found that in the irradiated MFP and lymph nodes (LN) 10 days after treatment, there was a significant increase in macrophages in immunocompetent mice and in mice with depleted $CD4^+$ T cells ($p<0.0001$). However, $CD8^+$ T cell levels did not change after RT, suggesting that normal tissue radiation leads to chemotactic signals for macrophages consistent with CCL3, 4, and 5 increases from MEFs in culture as well as CCL3 and CCL4 enhancement after *ex vivo* MFP irradiation (Fig. 4A–D and Supplementary Fig. S7A–D). Macrophage infiltration was further increased after $CD8^+$ T cell depletion (2-fold, $p<0.0001$), suggesting the magnitude of macrophage recruitment is T cell dependent. IHC staining for $F4/80^+$ cells in Nu/Nu mice confirmed an increase in macrophage infiltration 10 days after RT (Supplementary Fig. S8A and S8B). We used flow cytometry to further quantify $CD11b^+F4/80^+$ macrophages in the MFP (Supplementary Fig. S8C–E), validating that irradiation of normal tissue resulted in increased macrophage infiltration in immunocompromised mice.

Immune cell recruitment kinetics

To determine the dynamics of immune cell infiltration into irradiated tissues, we evaluated the time course of $CD8^+$ T cell and $F4/80^+$ macrophage infiltration after RT. While $CD8^+$ T cell levels remained unchanged in the MFP, they decreased significantly 1 day following RT ($p<0.001$) and recovered after 5 days in the ipsilateral inguinal LN (Supplementary Fig. S9A and S9B). In immunocompetent mice, macrophage infiltration was significantly enhanced in the MFP at 5 days post-RT ($p<0.05$) and in the LN at 1 day post-RT ($p<0.05$) (Fig. 4E and 4F). When $CD8^+$ T cells were depleted, $F4/80^+$ macrophage infiltration was significantly enhanced in the MFP at 5 days post-RT ($p<0.01$) and increased 2-fold in both the MFP and LN 10 days following RT ($p<0.0001$) when compared to the infiltration in

immunocompetent mice. Taken together, this suggests that functional $CD8^+$ T cell populations are necessary to prevent excess macrophage infiltration following RT.

Tumor cell invasion and chemotaxis

Due to the significant increase in $F4/80^+$ cell infiltration in the MFP 10 days after RT in the absence of $CD8^+$ T cells, we evaluated whether macrophages were directly responsible for tumor cell invasion. We isolated primary bone derived macrophages (BMDM) from both Nu/Nu and BALB/c mice. CM was collected after 48 hours and used in a transwell assay. CM from BMDMs of both mouse strains significantly enhanced 4T1 cell chemotaxis and invasion as compared to complete media alone (Supplementary Fig. S10A and S10B), indicating that the enhanced macrophage recruitment to irradiated tissues results in tumor cell recruitment. To identify the soluble factors responsible for tumor cell invasion *in vitro*, we performed a Luminex immunoassay on the CM, and it was found that CCL4 was the highest secreted chemokine (Supplementary Fig. S10C). In order to test if CCL4 was the factor that was enhancing tumor cell invasion, we blocked CCL4 with a neutralizing antibody (Supplementary Fig. S9A and S9B). Blocking CCL4 abrogated 4T1 invasion (4-fold, $p<0.05$) and chemotaxis (1.5-fold, $p<0.05$) while the addition of recombinant CCL4 enhanced 4T1 invasion (9-fold compared to complete media, $p<0.001$), suggesting that CCL4 secreted from macrophages in the MFP attract circulating tumor cells. To test whether local blockage of CCL4 could alter tumor cell recruitment *in vivo*, we locally administered a CCL4 blocking antibody to the MFP, which significantly decreased tumor cell recruitment to irradiated MFPs (Supplementary Fig. S10D).

Association between immune cell infiltration and tumor cell recruitment to irradiated normal tissues

CCL4 binds to the CCR5 receptor; to evaluate the relationship between macrophage and tumor cell infiltration into irradiated tissues, CCL4 activity was inhibited *in vivo* using maraviroc, an FDA approved CCR5 antagonist (27). Although maraviroc was initially approved for the treatment of HIV infection, it has been reported to influence macrophage and monocyte migration as well as cancer cell metastasis (25, 28). Blocking CCR5 has been shown to prevent invasion of multiple breast cancer cell lines *in vitro* and reduce pulmonary metastasis of MDA-MB-231 breast cancer cells in NOD/SCID mice (29). Strikingly, maraviroc treatment prevented tumor cell recruitment to irradiated normal tissues 10 days after RT in BALB/c mice with depleted $CD8^+$ T cells and Nu/Nu immunocompromised mice (Fig. 4G and Supplementary Fig. S8F). Maraviroc administration had no effect on tumor growth or lung metastasis in our model (Supplementary Fig. S3D–F and Supplementary Fig. S8G). IHC confirmed that infiltration of macrophages to irradiated MFPs and LNs was also attenuated 10 days after irradiation in mice treated with maraviroc (Fig. 4H and 4I), supporting the critical role of CCR5 in macrophage and tumor cell recruitment following RT. Because maraviroc reduces macrophage infiltration but does not deplete the population, we also administered clodronate liposomes, which have been used to specifically eliminate phagocytic cells through apoptosis (20). We confirmed that macrophage depletion results in reduced tumor cell recruitment to irradiated tissues (Supplementary Fig. S10D).

We determined changes in secreted factors in plasma 10 days after radiation compared to non-irradiated levels in immunocompetent and $CD8^+$ T cell depleted mice with or without maraviroc treatment using the Luminex immunoassay (Supplementary Fig. S11). Macrophage colony stimulating factor (MCSF) and the macrophage-produced interleukin 1-α (IL-1α) and macrophage inflammatory protein-2 (MIP2) secretion was higher in the plasma of $CD8^+$ T cell-depleted mice; moreover, this enhancement was abrogated by maraviroc treatment (30). This data provides a molecular underpinning for enhanced macrophage infiltration and for $CD8^+$ T cell prevention of excessive secretion of macrophage-promoting factors that enhance the infiltration and proliferation of macrophages. Our data suggests that irradiation of normal tissues promotes the secretion of CCL3, 4, and 5 by stromal cells, which increases macrophage migration. In the presence of $CD8^+$ T cells, further macrophage recruitment is prevented. However, in the absence of $CD8^+$ T cells, macrophages continue to infiltrate irradiated tissues, creating a positive feedback loop, which enhances CCL4 secretion and further attracts macrophages that promote tumor cell recruitment (Fig. 5). Blockade of CCR5, the receptor of CCL3, 4, and 5, prevents the enhancement of macrophage and tumor cell recruitment and rescues $CD8^+$ T cell depleted mice from tumor cell metastasis to irradiated tissues.

Discussion

The impact of the normal tissue response to RT and the resulting tumor cell migration may be important in a subset of breast cancer patients, particularly if patients have depressed ALCs. We identified a high risk TNBC group and showed that lymphocyte count is strongly associated with long term outcomes in these patients (Fig. 1A–F). To investigate the mechanism of this observation, we developed a mouse model of tumor cell recruitment to irradiated sites and found that irradiated tissues stimulate tumor cell migration in immunocompromised mice whereas this phenomenon does not occur in immunocompetent mice (Fig. 2A–F; Fig. 3A–I). Depletion of $CD8^+$ T cells significantly enhanced tumor cell establishment at irradiated sites, indicating that they normally function to inhibit tumor cell seeding. We noted increased macrophage infiltration after irradiation that was enhanced in the absence of $CD8^+$ T cells (Fig. 4A–I). *In vitro* studies indicated that the irradiated stroma secretes CCL3, 4, and 5, enhancing macrophage infiltration. Infiltrating macrophages secrete additional CCL4, which directly promotes tumor cell migration. *In vivo*, blocking the CCL3, 4, and 5 receptor, CCR5, using maraviroc prevented both enhanced macrophage infiltration of irradiated tissues and, consequently, tumor cell migration. We propose that in the absence of $CD8^+$ T cells, increased macrophage infiltration and thus CCL4 secretion results in a positive feedback loop of enhanced macrophage infiltration that then leads to tumor cell recruitment (Fig. 5). This agrees with clinical data showing that the presence of $CD8^+$ T cells in tumors and stroma is associated with a reduction in breast cancer mortality and enhanced stromal lymphocytic infiltrates are positively correlated with disease free survival and overall survival in TNBC (31–33).

Following ionizing radiation, macrophages are recruited to injured and irradiated tissues as part of the normal tissue radiation response (34). Furthermore, it is known that the presence of some populations of inflammatory macrophages is linked to poor outcomes and recurrence (35). Inflammatory $CD11b^+F4/80^+$ macrophages are recruited not only to the

pre-metastatic niche but also to circulating metastatic cells as they begin extravasation (36). These findings are consistent with our model in which tumor cell recruitment to irradiated tissues does not occur in the absence of macrophage infiltration. In addition, an inverse relationship between tumor associated macrophage density in the stroma and $CD8^+$ T cell infiltration has been reported in human breast tissues, and increased macrophage recruitment was shown to enhance primary tumor development and metastasis (37). Taken together with our data, these findings suggest that $CD8^+$ T cells modulate both tumor cell and macrophage recruitment.

We have identified a potential therapeutic strategy of using maraviroc following RT to prevent excessive macrophage infiltration in patients with persistent low lymphocyte counts. A variety of macrophage-targeted therapies has been developed and may potentially be applied toward overcoming poor outcomes associated with lymphopenia in breast cancer patients (37, 38). This therapeutic approach focuses on the downstream effects of lymphopenia rather than lymphopenia itself, such as through adoptive T cell transfer, which may have limited efficacy in stably increasing lymphocyte levels (9, 39).

We aimed to reproduce the conditions for locoregional tumor recurrence in TNBC patients with low lymphocyte counts following RT. Our model is not without limitations. Our pre-clinical model does not precisely recapitulate the clinical situation as we irradiated contralateral normal MFPs rather than MFPs of resected tumor sites in order to distinguish between the effects of radiation from those of wound healing, which can also affect tumor cell migration (40). As normal tissue is not spared in clinical radiation therapy, we aimed to determine the effects of radiation alone on tumor cell recruitment. In addition, a single dose as opposed to fractionated doses was used given the limited time frame of the model due to aggressive metastasis. However, we showed that tumor cell recruitment is dose-dependent (Supplementary Fig. S2), suggesting that the effect would be present if multiple doses were given. We also used luciferase-labeled cells in our studies, which may alter tumor and immune cell dynamics due to potential immunogenicity. However, orthotopic implantation of our luciferase-labeled 4T1 cells in Nu/Nu or BALB/c mice do not show differences in tumor growth rates (Figs. 3C and Supplementary Fig. S3A), minimizing the effect of luciferase incorporation. These limitations aside, our orthotopic model recapitulates the effects of immune status on local tumor recurrence following radiation as was found in our patient cohort.

Despite aggressive surgery, chemotherapy, and radiation treatment, TNBC patients are at an increased risk of locoregional recurrence, including patients who underwent a complete mastectomy and had no evidence of primary disease (41). This indicates that tumor cell recruitment of circulating tumor cells may be a contributing factor to recurrence as opposed to tumor cell persistence in the irradiated surgical bed. Other mechanisms may contribute to local recurrence following RT. Ahn et al. demonstrated that when tumors and surrounding normal tissue are irradiated, tumors use the vasculogenesis pathway to compensate for depleted vasculature to enable tumor regrowth and recurrence (42). $CD11b^+$ myeloid cell infiltration has been shown to contribute to tumor regrowth and metastasis progression (42, 43). In addition, studies employing pre-irradiation of the MFP to understand normal tissue influence on breast cancer progression and metastasis show breast tumor cell invasion

enhancement into surrounding muscle and fat due to pro-inflammatory factors released by injured stroma and $CD11b^+$ myeloid cell recruitment (44–47). Our work agrees with these results and suggests an effect of $CD11b^+$ macrophages in facilitating recurrence in patients with depressed levels of $CD8^+$ T cells following RT.

Our work demonstrates the importance of considering a personalized medicine approach to cancer therapy by observing tumor subtype and immune function when assessing failure and outcome risks. In cases involving TNBC combined with low lymphocyte count after RT, modified or additional treatment regimens that may improve local control are warranted. The radiation-induced increase in macrophage infiltration in the absence of $CD8^+$ T cells indicates their importance in preventing tumor cell recruitment. These results suggest that normal tissue radiation response may facilitate tumor cell invasion and recurrence in higher risk patients with low lymphocyte counts following RT.

Supplementary Material

Refer to Web version on PubMed Central for supplementary material.

Acknowledgments

The authors thank Dr. Duaa H. Al-Rawi for critical evaluation of the manuscript. We thank Drs. Nitin Raj and Laura D. Attardi for generously providing primary MEFs, Dr. Kerriann Casey for her analysis of potential off-target radiation effects in mice, and Ms. Tina Seto for providing data from the Oncoshare Project database. This research was financially supported by the Katherine McCormick Advanced Postdoctoral Fellowship and NIH grant# K99CA201304 (M. Rafat), the Ruth L. Kirschstein National Research Service Award PA-14-015 Grant# T32CA121940 (M. Rafat and T. A. Aguilera), the Susan and Richard Levy Gift Fund; the Suzanne Pride Bryan Fund for Breast Cancer Research; the Breast Cancer Research Foundation; the Regents of the University of California's California Breast Cancer Research Program (16OB-0149 and 19IB-0124); the Stanford University Developmental Research Fund; and the National Cancer Institute's Surveillance, Epidemiology and End Results Program under contractHHSN261201000140C awarded to the Cancer Prevention Institute of California. The project was supported by an NIH CTSA award number UL1 RR025744. The collection of cancer incidence data used in this study was supported by the California Department of Health Services as part of the statewide cancer reporting program mandated by California Health and Safety Code Section 103885; the National Cancer Institute's Surveillance, Epidemiology, and End Results Program under contract HHSN261201000140C awarded to the Cancer Prevention Institute of California, contract HHSN261201000035C awarded to the University of Southern California, and contract HHSN261201000034C awarded to the Public Health Institute; and the Centers for Disease Control and Prevention's National Program of Cancer Registries, under agreement #1U58 DP000807-01 awarded to the Public Health Institute. The ideas and opinions expressed herein are those of the authors, and endorsement by the University or State of California, the California Department of Health Services, the National Cancer Institute, or the Centers for Disease Control and Prevention or their contractors and subcontractors is not intended nor should be inferred.

References

1. Sioshansi S, Ehdaivand S, Cramer C, Lomme MM, Price LL, Wazer DE. Triple negative breast cancer is associated with an increased risk of residual invasive carcinoma after lumpectomy. Cancer. 2012; 118:3893–8. [PubMed: 22864932]
2. Lowery AJ, Kell MR, Glynn RW, Kerin MJ, Sweeney KJ. Locoregional recurrence after breast cancer surgery: a systematic review by receptor phenotype. Breast Cancer Res Treat. 2012; 133:831–41. [PubMed: 22147079]
3. Whelan TJ, Pignol JP, Levine MN, Julian JA, MacKenzie R, Parpia S, et al. Long-term results of hypofractionated radiation therapy for breast cancer. N Engl J Med. 2010; 362:513–20. [PubMed: 20147717]

4. Simone NL, Dan T, Shih J, Smith SL, Sciuto L, Lita E, et al. Twenty-five year results of the national cancer institute randomized breast conservation trial. Breast Cancer Res Treat. 2012; 132:197–203. [PubMed: 22113254]
5. Parikh RR, Housman D, Yang Q, Toppmeyer D, Wilson LD, Haffty BG. Prognostic value of triple-negative phenotype at the time of locally recurrent, conservatively treated breast cancer. Int J Radiat Oncol Biol Phys. 2008; 72:1056–63. [PubMed: 18676094]
6. Li J, Gonzalez-Angulo AM, Allen PK, Yu TK, Woodward WA, Ueno NT, et al. Triple-negative subtype predicts poor overall survival and high locoregional relapse in inflammatory breast cancer. Oncologist. 2011; 16:1675–83. [PubMed: 22147002]
7. Pogoda K, Niwinska A, Murawska M, Pienkowski T. Analysis of pattern, time and risk factors influencing recurrence in triple-negative breast cancer patients. Med Oncol. 2013; 30:388. [PubMed: 23292831]
8. Conesa MAVC, Garcia-Martinez E, Billalabeitia EG, Benito AC, Garcia TG, Garcia VV, et al. Predictive value of peripheral blood lymphocyte count in breast cancer patients treated with primary chemotherapy. The Breast. 2012; 21:468–74. [PubMed: 22119767]
9. Kuo P, Bratman SV, Shultz DB, von Eyben R, Chan C, Wang Z, et al. Galectin-1 mediates radiation-related lymphopenia and attenuates NSCLC radiation response. Clin Cancer Res. 2014; 20:5558–69. [PubMed: 25189484]
10. Afghahi A, Mathur M, Seto T, Desai M, Kenkare P, Horst KC, et al. Lymphopenia after adjuvant radiotherapy (RT) to predict poor survival in triple-negative breast cancer (TNBC). J Clin Oncol. 2015; 33(Suppl) abstr 1069.
11. Ebctcg, McGale P, Taylor C, Correa C, Cutter D, Duane F, et al. Effect of radiotherapy after mastectomy and axillary surgery on 10-year recurrence and 20-year breast cancer mortality: meta-analysis of individual patient data for 8135 women in 22 randomised trials. Lancet. 2014; 383:2127–35. [PubMed: 24656685]
12. Vilalta M, Rafat M, Giaccia AJ, Graves EE. Recruitment of circulating breast cancer cells is stimulated by radiotherapy. Cell Rep. 2014; 8:402–9. [PubMed: 25017065]
13. Moran MS. Radiation therapy in the locoregional treatment of triple-negative breast cancer. Lancet Oncol. 2015; 16:e113–22. [PubMed: 25752562]
14. Kurian AW, Mitani A, Desai M, Yu PP, Seto T, Weber SC, et al. Breast cancer treatment across health care systems: linking electronic medical records and state registry data to enable outcomes research. Cancer. 2014; 120:103–11. [PubMed: 24101577]
15. Weber SC, Seto T, Olson C, Kenkare P, Kurian AW, Das AK. Oncoshare: lessons learned from building an integrated multi-institutional database for comparative effectiveness research. AMIA Annu Symp Proc. 2012; 2012:970–8. [PubMed: 23304372]
16. Lu L, Xu X, Zhang B, Zhang R, Ji H, Wang X. Combined PD-1 blockade and GITR triggering induce a potent antitumor immunity in murine cancer models and synergizes with chemotherapeutic drugs. J Transl Med. 2014; 12:36. [PubMed: 24502656]
17. Mencarelli A, Graziosi L, Renga B, Cipriani S, D'Amore C, Francisci D, et al. CCR5 Antagonism by Maraviroc Reduces the Potential for Gastric Cancer Cell Dissemination. Transl Oncol. 2013; 6:784–93. [PubMed: 24466382]
18. Castellino F, Huang AY, Altan-Bonnet G, Stoll S, Scheinecker C, Germain RN. Chemokines enhance immunity by guiding naive CD8+ T cells to sites of CD4+ T cell-dendritic cell interaction. Nature. 2006; 440:890–5. [PubMed: 16612374]
19. Brewitz A, Eickhoff S, Dahling S, Quast T, Bedoui S, Kroczek RA, et al. CD8(+) T Cells Orchestrate pDC-XCR1(+) Dendritic Cell Spatial and Functional Cooperativity to Optimize Priming. Immunity. 2017; 46:205–19. [PubMed: 28190711]
20. van Rooijen N, Hendrikx E. Liposomes for specific depletion of macrophages from organs and tissues. Methods Mol Biol. 2010; 605:189–203. [PubMed: 20072882]
21. Ying W, Cheruku PS, Bazer FW, Safe SH, Zhou B. Investigation of macrophage polarization using bone marrow derived macrophages. J Vis Exp. 2013
22. Ward ST, Li KK, Hepburn E, Weston CJ, Curbishley SM, Reynolds GM, et al. The effects of CCR5 inhibition on regulatory T-cell recruitment to colorectal cancer. Br J Cancer. 2015; 112:319–28. [PubMed: 25405854]

23. Ray-Coquard I, Cropet C, Van Glabbeke M, Sebban C, Le Cesne A, Judson I, et al. Lymphopenia as a prognostic factor for overall survival in advanced carcinomas, sarcomas, and lymphomas. Cancer Res. 2009; 69:5383–91. [PubMed: 19549917]
24. Lazennec G, Richmond A. Chemokines and chemokine receptors: new insights into cancer-related inflammation. Trends Mol Med. 2010; 16:133–44. [PubMed: 20163989]
25. Weitzenfeld P, Ben-Baruch A. The chemokine system, and its CCR5 and CXCR4 receptors, as potential targets for personalized therapy in cancer. Cancer Lett. 2014; 352:36–53. [PubMed: 24141062]
26. Balkwill F. Cancer and the chemokine network. Nat Rev Cancer. 2004; 4:540–50. [PubMed: 15229479]
27. Gouwy M, Struyf S, Berghmans N, Vanormelingen C, Schols D, Van Damme J. CXCR4 and CCR5 ligands cooperate in monocyte and lymphocyte migration and in inhibition of dual-tropic (R5/X4) HIV-1 infection. Eur J Immunol. 2011; 41:963–73. [PubMed: 21381021]
28. Rossi R, Lichtner M, De Rosa A, Sauzullo I, Mengoni F, Massetti AP, et al. In vitro effect of anti-human immunodeficiency virus CCR5 antagonist maraviroc on chemotactic activity of monocytes, macrophages and dendritic cells. Clin Exp Immunol. 2011; 166:184–90. [PubMed: 21985364]
29. Velasco-Velazquez M, Jiao X, De La Fuente M, Pestell TG, Ertel A, Lisanti MP, et al. CCR5 antagonist blocks metastasis of basal breast cancer cells. Cancer Res. 2012; 72:3839–50. [PubMed: 22637726]
30. Arango Duque G, Descoteaux A. Macrophage Cytokines: Involvement in Immunity and Infectious Diseases. Front Immunol. 2014; 5:1–12. [PubMed: 24474949]
31. Ali HR, Provenzano E, Dawson SJ, Blows FM, Liu B, Shah M, et al. Association between CD8+ T-cell infiltration and breast cancer survival in 12,439 patients. Ann Oncol. 2014; 25:1536–43. [PubMed: 24915873]
32. Adams S, Gray RJ, Demaria S, Goldstein L, Perez EA, Shulman LN, et al. Prognostic value of tumor-infiltrating lymphocytes in triple-negative breast cancers from two phase III randomized adjuvant breast cancer trials: ECOG 2197 and ECOG 1199. J Clin Oncol. 2014; 32:2959–66. [PubMed: 25071121]
33. Gentles AJ, Newman AM, Liu CL, Bratman SV, Feng W, Kim D, et al. The prognostic landscape of genes and infiltrating immune cells across human cancers. Nat Med. 2015; 21:938–45. [PubMed: 26193342]
34. Denham JW, Hauer-Jensen M. The radiotherapeutic injury--a complex 'wound'. Radiother Oncol. 2002; 63:129–45. [PubMed: 12063002]
35. Medrek C, Ponten F, Jirstrom K, Leandersson K. The presence of tumor associated macrophages in tumor stroma as a prognostic marker for breast cancer patients. BMC Cancer. 2012; 12:306. [PubMed: 22824040]
36. Qian B, Deng Y, Im JH, Muschel RJ, Zou Y, Li J, et al. A distinct macrophage population mediates metastatic breast cancer cell extravasation, establishment and growth. PLoS One. 2009; 4:e6562. [PubMed: 19668347]
37. DeNardo DG, Brennan DJ, Rexhepaj E, Ruffell B, Shiao SL, Madden SF, et al. Leukocyte complexity predicts breast cancer survival and functionally regulates response to chemotherapy. Cancer Discov. 2011; 1:54–67. [PubMed: 22039576]
38. Chaudary N, Pintilie M, Jelveh S, Lindsay P, Hill RP, Milosevic M. Plerixafor Improves Primary Tumor Response and Reduces Metastases in Cervical Cancer Treated with Radio-Chemotherapy. Clin Cancer Res. 2017; 23:1242–49. [PubMed: 27697997]
39. Muranski P, Boni A, Wrzesinski C, Citrin DE, Rosenberg SA, Childs R, et al. Increased intensity lymphodepletion and adoptive immunotherapy--how far can we go? Nat Clin Pract Oncol. 2006; 3:668–81. [PubMed: 17139318]
40. Coussens LM, Werb Z. Inflammation and cancer. Nature. 2002; 420:860–7. [PubMed: 12490959]
41. Voduc KD, Cheang MC, Tyldesley S, Gelmon K, Nielsen TO, Kennecke H. Breast cancer subtypes and the risk of local and regional relapse. J Clin Oncol. 2010; 28:1684–91. [PubMed: 20194857]
42. Ahn GO, Tseng D, Liao CH, Dorie MJ, Czechowicz A, Brown JM. Inhibition of Mac-1 (CD11b/CD18) enhances tumor response to radiation by reducing myeloid cell recruitment. Proc Natl Acad Sci U S A. 2010; 107:8363–8. [PubMed: 20404138]

43. DeNardo DG, Barreto JB, Andreu P, Vasquez L, Tawfik D, Kolhatkar N, et al. CD4(+) T cells regulate pulmonary metastasis of mammary carcinomas by enhancing protumor properties of macrophages. Cancer Cell. 2009; 16:91–102. [PubMed: 19647220]

44. Lemay R, Archambault M, Tremblay L, Bujold R, Lepage M, Paquette B. Irradiation of normal mouse tissue increases the invasiveness of mammary cancer cells. Int J Radiat Biol. 2011; 87:472–82. [PubMed: 21231833]

45. Kuonen F, Laurent J, Secondini C, Lorusso G, Stehle JC, Rausch T, et al. Inhibition of the Kit ligand/c-Kit axis attenuates metastasis in a mouse model mimicking local breast cancer relapse after radiotherapy. Clin Cancer Res. 2012; 18:4365–74. [PubMed: 22711708]

46. Bouchard G, Bouvette G, Therriault H, Bujold R, Saucier C, Paquette B. Pre-irradiation of mouse mammary gland stimulates cancer cell migration and development of lung metastases. Br J Cancer. 2013; 109:1829–38. [PubMed: 24002607]

47. Bouchard G, Therriault H, Geha S, Berube-Lauziere Y, Bujold R, Saucier C, et al. Stimulation of triple negative breast cancer cell migration and metastases formation is prevented by chloroquine in a pre-irradiated mouse model. BMC Cancer. 2016; 16:361. [PubMed: 27282478]

Significance

This study establishes the importance of macrophages in driving tumor cell recruitment to sites of local radiation therapy and suggests that this mechanism contributes to local recurrence in women with TNBC that are also immunosuppressed.

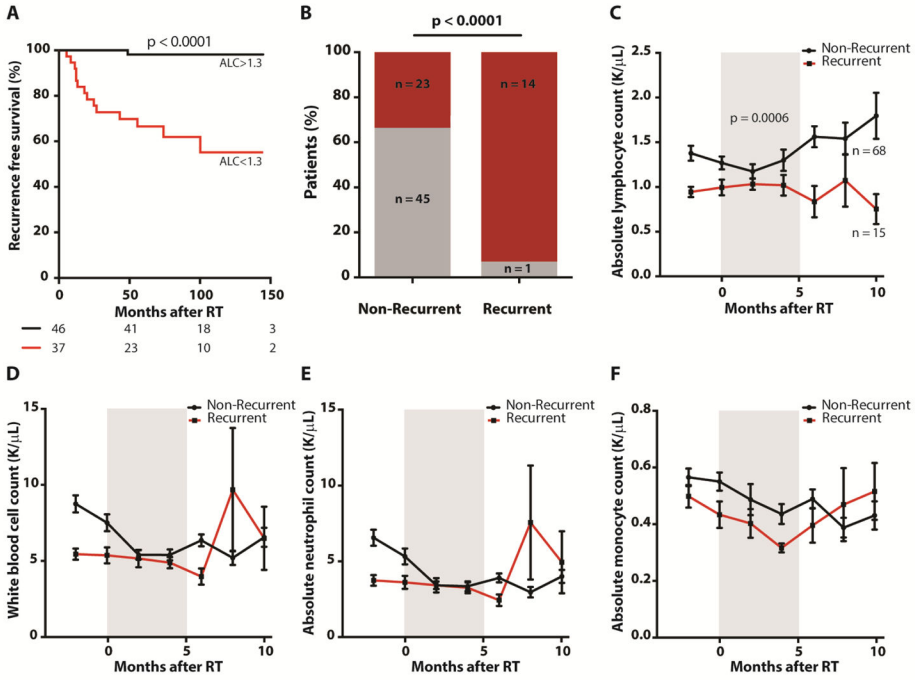

Figure 1.

Low absolute lymphocyte count after RT predicts locoregional recurrence in TNBC patients. **A,** Kaplan-Meier analysis of recurrence free survival based on ALC (black line, ALC>1.3K/μL; red line, ALC<1.3K/μL up to 5 months following RT). At risk subjects are indicated along the x-axis. Statistical significance was determined using the Log-rank test. **B,** Recurrent (n = 15) and non-recurrent (n = 68) patients with low ALC following RT. Red bars indicate patients with ALC<1.3K/μL 1 to 5 months following RT while gray bars indicate ALC>1.3K/μL over the same time period. Statistical significance was determined using Fisher's exact test. **C,** Sustained low ALC 1 to 5 months after RT in recurrent (red line) compared to non-recurrent (black line) patients. White blood cell (**D**), absolute neutrophil (**E**), and absolute monocyte count (**F**) 1 to 5 months after RT in recurrent (red line) compared to non-recurrent (black line) patients. Gray shading from 0–5 months after RT in cell count figures indicate ALC evaluation timeframe. Error bars show standard error mean. Statistical significance was determined using a repeated measures model.

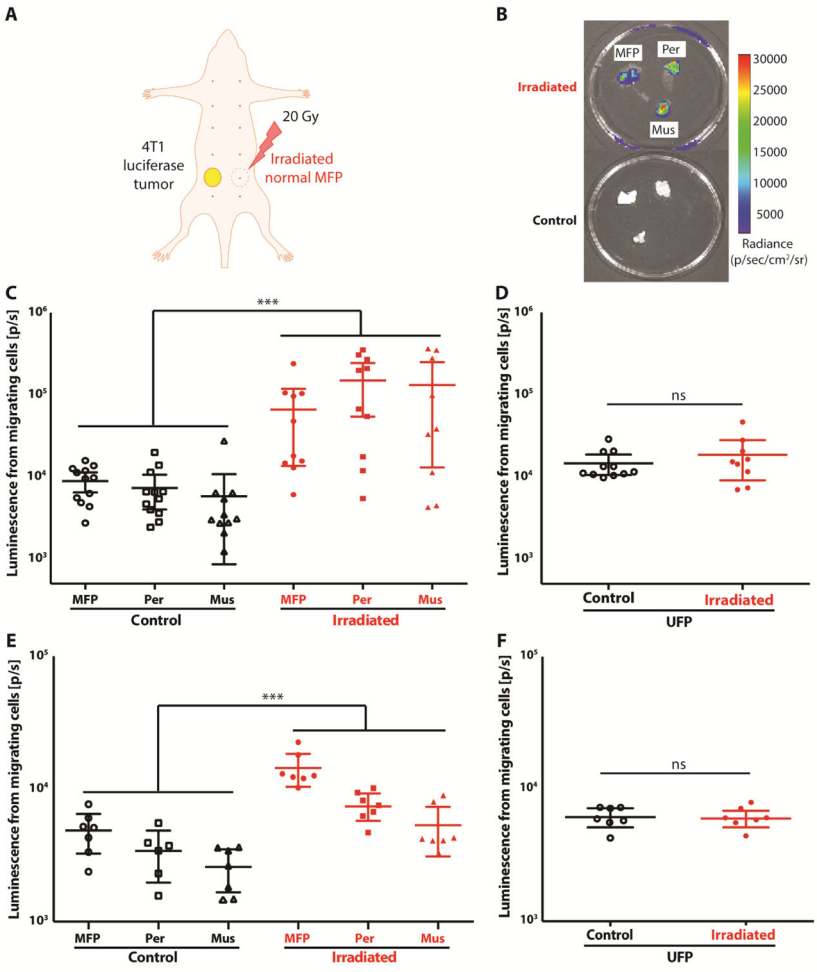

Figure 2.

Irradiation of normal tissues promotes tumor cell recruitment *in vivo* in Nu/Nu mice. **A,** Experimental schematic. **B,** Representative BLI image of irradiated (20 Gy) and control unirradiated (0 Gy) mammary fat pad (MFP), peritoneum (Peri), and muscle (mus) tissues in the radiation field outlined by the dashed circle in (A). **C,** Tumor cell migration following RT in the 4T1 model (n = 12, control; n = 10, irradiated) with corresponding upper MFP (UFP) tissues collected from unirradiated control or irradiated mice, which are outside of the radiation field to test whether tumor cell recruitment was localized to the irradiated areas (**D**). **E,** MDA-MB-231 model (n = 7 control; n = 7 irradiated) with corresponding UFP control (**F**). Statistical significance was determined by ANOVA analysis with ***p<0.001. Error bars show the 95% confidence limit.

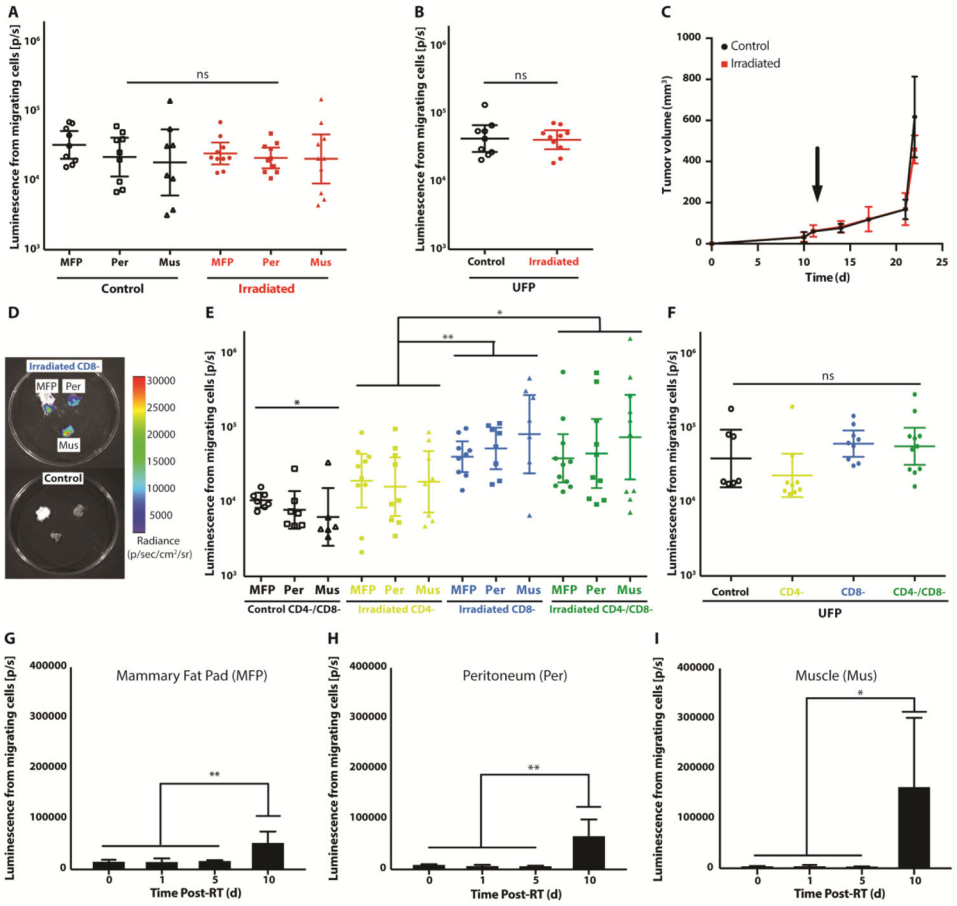

Figure 3.

Irradiation of normal tissues promotes tumor cell migration *in vivo* upon T cell depletion in BALB/c mice. **A,** 4T1 cell infiltration in the MFP, peritoneum (Per), and muscle (Mus) 10 days following RT at 20 Gy (n = 9, control; n = 10, irradiated) in immunocompetent BALB/c mice. **B,** BLI signal from control upper MFPs (UFP) outside of the radiation field in immunocompetent mice. **C,** 4T1 primary tumor growth curves in mice with control and irradiated contralateral MFPs. Arrow indicates time of RT of normal MFP. **D,** Representative BLI image of irradiated and control tissues after T cell depletion. **E,** Tumor cell migration following $CD4^+$ (n = 9, $CD4^-$) and $CD8^+$ (n = 8, $CD8^-$) T cell depletion individually or in combination (n = 10) 10 days after RT. Statistical significance was found between the control (n = 7) and irradiated conditions (*$p<0.05$), but the irradiated $CD8^-$ condition was not significantly different from the combination treatment. **F,** BLI signal from control UFPs outside of the radiation field in mice with depleted T cell populations. Kinetics of tumor cell recruitment to MFP (**G**), Per (**H**), and Mus (**I**) tissues in mice with depleted $CD8^+$ T cells using BLI (n = 6, 0–5 days post-RT; n = 8, 10 days post-RT). Statistical significance was determined by ANOVA analysis with *$p<0.05$ and **$p<0.01$. Error bars show the 95% confidence limit.

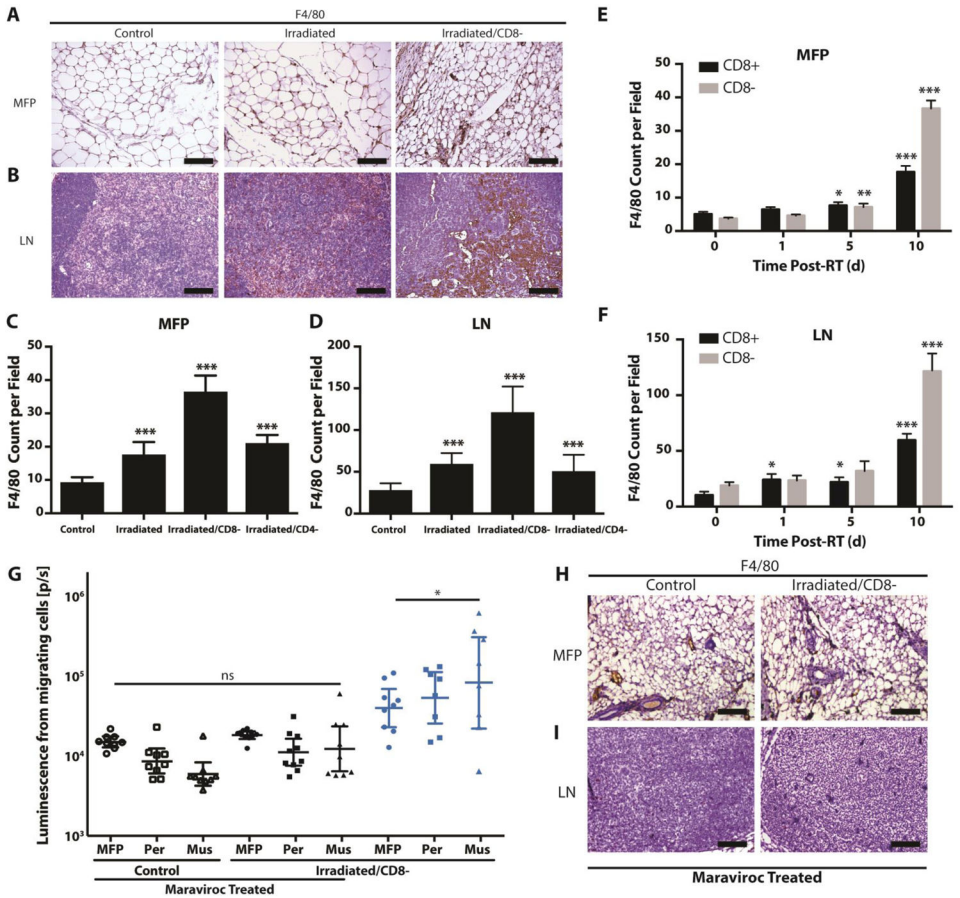

Figure 4.

Immune cell infiltration in normal tissues. Immunohistochemistry (IHC) was performed to detect infiltrating F4/80$^+$ macrophages in BALB/c mice with (n = 10) and without (n = 8) CD8$^+$ T cells in irradiated (20 Gy) and control (n = 9, 0 Gy) MFP (**A**) and lymph nodes (**B**, LN) 10 days after RT. The corresponding quantification in addition to F4/80$^+$ macrophage counts in mice with CD4$^+$ T cell depletion (n = 9) is shown in the MFP (**C**) and LN (**D**). Statistical significance in F4/80$^+$ infiltration experiments was determined in comparison to unirradiated control tissues. Time course of F4/80$^+$ macrophage cell infiltration in control and irradiated MFP (**E**) and LN (**F**) (n = 6, 0–5 days post-RT; n = 10, CD8$^+$ 10 days post-RT; n = 8, CD8$^-$ 10 days post-RT). Statistical significance in F4/80$^+$ time course experiments determined in comparison to baseline infiltration 0 days post-RT. Error bars show 95% confidence limit with *p<0.05, **p< 0.01, and ***p<0.0001 as determined by a two-tailed unpaired t-test. **G,** BLI was used to show that tumor cell migration is mitigated in BALB/c mice without CD8$^+$ T cells following RT at 20 Gy using maraviroc to block the CCR5 receptor (n = 9, unirradiated and n = 10, irradiated with maraviroc treatment; n = 9, irradiated without maraviroc treatment from Figure 3E). Error bars show the 95% confidence limit with *p<0.05 as determined by ANOVA analysis. Statistical significance was found when comparing the irradiated tissues without maraviroc treatment to the irradiated and control tissues with maraviroc treatment. The decrease in macrophage

migration was confirmed using IHC in the MFP (**H**) and LN (**I**) of unirradiated and irradiated mice with depleted $CD8^+$ T cells. Scale bar is 100μm.

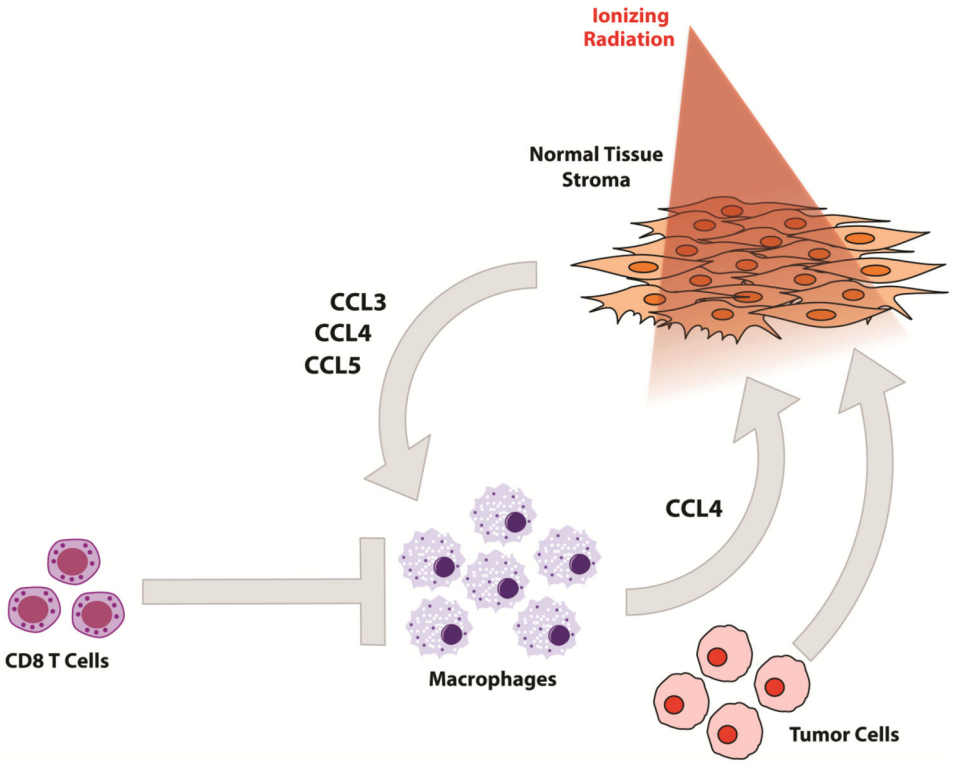

Figure 5.

Model of tumor cell recruitment into irradiated tissues in the absence or presence of $CD8^+$ T cells. Radiation of normal tissue induces stromal secretion of chemokines that induce macrophage infiltration. Suppressed $CD8^+$ T cell levels allow excess macrophage infiltration that causes more secretion of chemokines that attract circulating tumor cells.

Table 1

Summary of tumor and treatment characteristics in patients stratified by recurrence or ALC.

	Recurrent	Non-Recurrent	ALC < 1.3	ALC > 1.3
No. Patients	15	68	37	46
	Median (range)	**Median (range)**	**Median (range)**	**Median (range)**
Age (y)	48 (26–77)	50.5 (26–87)	48 (26–77)	52.5 (31–87)
Follow-up (months)	53 (20–169)	82 (16–176)	73 (16–169)	84.5 (29–176)
Stage Distribution	**%**	**%**	**%**	**%**
I	20.0	20.6	18.9	21.7
II	33.3	57.4	43.2	60.9
III	46.7	22.1	37.8	17.4
Nodal Status	**%**	**%**	**%**	**%**
Positive	66.7	38.2	54.1	34.8
Negative	33.3	61.8	45.9	65.2
Chemotherapy	86.7	92.6	91.9	93.5
Surgery	**%**	**%**	**%**	**%**
Mastectomy	40.0	29.4	35.1	28.3
Lumpectomy	60.0	70.6	64.9	71.7
Mortality	53.3	10.3	27.0	10.9